American Journal of Molecular Biology, 2015, 5, 105-116
Published Online July 2015 in SciRes. http://www.scirp.org/journal/ajmb
http://dx.doi.org/10.4236/ajmb.2015.53009

AMPK Subcellular Localisation in *Dictyostelium discoideum*

Paul B. Bokko[1,2], Afsar Ahmed[1,3], Paul R. Fisher[1]

[1]School of Life Sciences, La Trobe University, Bundoora, Australia
[2]Department of Veterinary Surgery and Theriogenology, University of Maiduguri, Maiduguri, Nigeria
[3]Monash Medical Research Institute, Monash University, Clayton, Australia
Email: bokkopx@yahoo.com

Received 21 March 2015; accepted 25 July 2015; published 28 July 2015

Abstract

The *Dictyostelium discoideum* AMP-activated protein kinase (AMPK) *snf*A subcellular localization was studied in AX2 and stable HPF strains by use of AMPK antipeptide antibody and goat anti-rabbit Alexa-Flour 488-conjugated IgG antibody. The AMPK exhibited cytosolic localization patterns and uniform focalised concentrations in wild type and the strains alike. Constitutive activation and attenuation of the *α* subunit expression did not affect subcellular distribution of AMPK. However, *snf*A expression was more intense in strains in which AMPK was constitutively active compared with the AX2 but lesser in attenuation strains. The localisation of the *snf*A reinforced the putative standing that it had a plethora of cytoplasmic functions. Moreover, the oxidative cellular function would require a ubiquitous system and might coordinately regulate responses to metabolic requirements. Furthermore, the developmental phases of the life cycle would support the cytosolic localization; and since organelles were potentially reorganized or removed entirely during the transition from vegetative living to fruiting body morphology. This study provided insight into the subcellular distribution of AMPK in *Dictyostelium discoideum*. We demonstrated that AMPK localization was steady in AX2 and derived strains whether constitutively active or antisense inhibited depicting extreme genetic states.

Keywords

AMPK *α* Subunit, *Dictyostelium discoideum*, Subcellular Localisation, AX2, Mitochondrial Assay

1. Introduction

Sucrose non-fermenting protein (*snf*)A/AMP-activated protein kinase (AMPK) ortholog are eukaryotic serine/

How to cite this paper: Bokko, P.B., Ahmed, A. and Fisher, P.R. (2015) AMPK Subcellular Localisation in *Dictyostelium discoideum*. *American Journal of Molecular Biology*, **5**, 105-116. http://dx.doi.org/10.4236/ajmb.2015.53009

threonine kinases that mediate cellular energy homeostasis [1] [2]. The enzyme cascade regulates cell growth, transcription and the cellular response to nutrient limitation and stress [3]-[5]. In *Dictyostelium*, each subunit isoform is encoded by a single gene [6] [7]. The *Dictyostelium* AMPK α subunit gene ortholog *snf*A, encodes a protein of 727 amino acids with a molecular weight of 81638.9 Da; and is located on chromosome 3 (position 589784 - 592434) of the *Dictyostelium* genome [6]. The *D. discoideum* AMPK α subunit is made up of 5 exons and 4 introns [7]. The Asparagine-rich domains such as that within the AMPK α sequence are prevalent in *Dictyostelium* proteins, but their functions are unknown [7]. The *D. discoideum* AMPK α subunit is structurally partitioned into four major domains namely: the catalytic domain, also known as serine-threonine kinase domain (S_TKc), composed of 254 residues (positions 31 - 284), contains the phosphorylation residue, Thr188 on the α-subunit, which can be mediated by upstream regulatory kinases; the KIS binding domain (residues 330 - 389, 630 - 727) that interacts with the β subunit and is interrupted by an intervening asparagine-rich (241 residues) domains inserted 98 amino acids upstream of the C-terminus) and the autoinhibitory region extending to the C-terminus [8]. The KIS binding domain and autoinhibitory regions are required for assembly of the α subunit into the heterotrimeric holoenzyme and regulation by the γ subunit respectively assembled on β subunit [7]. These domains of AMPK α subunit are features shared by AMPK α subunit or their homologues in other eukaryotes showing that the AMPK α subunit is highly conserved in eukaryotes [9]. To date, little is known about precise subcellular localization of *snf*A within cell and how its intracellular distribution is controlled. This knowledge is important, because it will set the stage to identify specific AMPK functions in compartments that are dictated by physiological changes.

2. Materials and Methods

2.1. *Dictyostelium discoideum*: Strains and Culture Conditions

All experiments were conducted with *D. discoideum* AX2 wild-type parental strain [10], and strains derived from it [7]. Each strain carried multiple copies of the following plasmid constructs: 1) pPROF362 (the AMPK α (*snf*A subunit antisense inhibition constructs) in HPF456-462; 2) pPROF361 (its corresponding RNA control construct in HPF466-468; or 3) pPROF 392 (the AMPK α^{380} overexpression construct) in HPF434-442 strains. All strains were isolated using the $Ca(PO_4)_2$/DNA coprecipitation method [11] and selected as isolated, independent colonies growing on *Micrococcus luteus* lawns on SM agar supplemented with 20 µg/mL geneticin (G-418) (Promega Corporation, Madison, WI). Strains of *Dictyostelium* were maintained as axenic cultures at 21˚C ± 1˚C in HL5 medium supplemented with 100 µg/mL ampicillin and 20 µg/mL streptomycin or on SM plates with *Klebsiella aerogenes* as a bacterial food source. The selective agent Geneticin (G418 @ 20 µg/mL) was added to HL5 medium for all strains. All localization experiments were performed on vegetative, exponentially growing cells.

2.2. Gene Cloning and Sequence Analysis

AMPK cloning strategies and vectors were as described previously [7]. The *snf*A [8]; EMBL/GenBank ID AF118151) encoding the AMPK α subunit was amplified from genomic DNA template using the gene-specific primers PAMKF1 P5' > GCGCTCTAGATTCGAAAAAATCATGAGTCCATATCAACAATAATCCCATT > 3'and PAMKR1 5' > GCGCTCTAGACTCGAGTTAAACTACAAATATCAAAAATATGAATATTTCACC > 3' [7] and cloned into $pZerO_2$ (Invitrogen, Carlsbad, CA). The amino acid sequences of AMPK α subunit gene used in this study had been earlier characterised [7].

2.3. Generation of Constitutively Active Form of AMPK α Subunit

The cDNA encoding the catalytic domain of AMPK α subunit consisting of 380 amino acid residues was amplified using PACDNAF1 5'-GCGCTCTAGAAGCTTCTCGAGTTCGAAATGAGTCCATATCAACAAAATCCCATTGG-3' and PACDNAR1A 5'-GCGCTCTAGACTCGAGCCCGGGAATTCTTATTGGCCTCT-GGGGAGCACTGACAT-3' primers by reverse transcription PCR (RT-PCR) from RNA extracted from vegetative AX2 using the RNAzol (Life Technologies Inc., Grand Island, NY). The amplified catalytic domain comprising 1140 bp cDNA fragment designated AMPK α^{380} was cloned into the *Xba*I-linearized pZErO^{TM}-2 thereafter subcloned into the *Cla*I-*Xho*I sites of the pA15GFP [12] [13] replacing the resident green fluorescent protein (GFP) gene, creating a fusion of the actin15 promoter-AMPK gene to yield pPROF 392 for overexpression of a constitutively

active, truncated AMPK α subunit. Localization of a fluorescently tagged protein expressed by the Act15 promoter with the markers has been used extensively to define subcellular localization [14] [15].

2.4. Creation of the AMPK α Subunit Antisense/Sense Constructs

Antisense inhibition offers partial inhibition of expression of essential genes producing sublethal phenotypes. Plasmid constructs for expression of antisense RNA and and the corresponding sense RNA control were created from the full length genomic clone (pPROF348) template by amplifying a fragment using primers PAMPKF10 [5'GCGCTCTAGAATTCCCTATGGATGAAAAGATTAGAAGA3'] and PAMPKR10 [5'GCGCTCTAGAATTCTCCATGCTATTGCTATTGGTGG3'], cloned into *Xba*I site of pZErO^{TM}-2 and subcloned into the *Eco*RI site of the *Dictyostelium* expression vector, pDNeo2 under the control of the actin 6 promoter [16] in both orientations. The resulting AMPK α sense (pPROF361) and antisense (pPROF362) constructs express 1172 bp of the AMPK α antisense RNA along with the corresponding sense RNA control. Both fragments would be expressed under the control of the *Dictyostelium* actin 6 promoter.

Sequences of PCR products and clones were verified by sequencing conducted through the Australian Genome Research Facility (AGRF), Brisbane, Australia.

2.5. Determination of Plasmid Copies and Estimation of RNA Expression in Strains by ECF Signal Amplification Method

Equal amounts of DNA (digested with *Eco*RI) or RNA from AX2 and each strain was used. The DNA and RNA resolution, transfer and hybridization for quantitative Southern and northern blotting were performed and employing the fluorescein-labelled DNA probe and liquid block. For enhanced chemifluorescent detection, the blot was incubated in 5000-fold dilution of anti-fluorescein AP-conjugate containing 0.5% (w/v) BSA in buffer A1 (0.32 mL/cm^2) with gentle agitation at room temperature for 1 hr and washed 3 × 10 min in 0.3% (v/v) Tween 20 in buffer A1 at room temperature with agitation and blot was scanned in the Storm860^{TM} Fluoroimager (Amersham Biosciences, Castle Hill, Sydney, Australia) using the 530 nm filter in fluorescence mode. The RFU values from each strain and serial dilutions of linear plasmid of known concentration as well as the RFU values from AX2 gDNA were analysed using the ImageQuant tool (TLv2003.03) software as the ratio of the RFU values of respective strain to the RFU values of AX2. The quantitative figures from the Southern blot enabled the computation of plasmid copy numbers for all strains tested whereas the signals from the northern blots were used for the computation of RNA expression levels in strains and AX2.

2.6. Mitochondrial "Mass" Estimation

MitoTracker green FM (Molecular Probes™ Inc., Eugene, OR, USA) selectively stains mitochondria in a manner that is independent of mitochondrial membrane potential. MitoTracker green fluorescence was therefore used as a measure of mitochondrial "mass". Axenically growing cells at the exponential phase was spun at 3000 x g for 15 sec, washed once and incubated in Lo-Flo HL-5 (3.85 g/L glucose, 1.78 g/L proteose peptone, 0.45 g/L yeast extract, 0.485 g/L KH_2PO_4 and 1.2 g/L $Na_2HPO_4{\cdot}12H_2O$; filter sterile) buffer for 2 hrs. An aliquot was resuspended in Lo-Flo HL-5 containing 200 nM MitoTracker green FM alongside an unstained control and incubated for an hour in the dark. The unbound MitoTracker green was removed by washing the cells 3 times with Lo-Flo HL-5 for 10 min on an orbital shaker (150 rpm). The cells were resuspended in Lo-Flo HL-5 and fluorescence was measured in duplicate in a fluorometer (Turner Biosystems Modulus™ Inc., Mary Ave. Sunnyvale CA, USA) using the Blue Module. The MitoTracker green fluorescence per million cells was calculated after subtraction of the background fluorescence as in the unstained cells. The correlation of MitoTracker green fluorescence intensity was tested against plasmid copies in the in overexpression and antisense-inhibited strains relative to AX2.

2.7. Mitochondrial Staining

Mitochondria location within the cell was assayed by use of MitoTracker Red (CMX-Ros, Molecular Probes™ Inc., Eugene, OR, USA). Briefly, 5 - 7 mL axenically growing culture cells at 2 × 10^6 cells/mL was deposited on sterile coverslips in the 6-well plates (Nalge Nunc™, Naperville, IL) and allowed to settle and adhere to the coverslip over a period of 4 - 6 hr. The cells were gently washed once in fresh Lo-Flo H-5 medium for 2 hrs.

One well was incubated only Lo-Flo HL5 as an unstained control. The cells adherent to the coverslip were stained with 200 nM MitoTracker Red (CMX-Ros, Molecular Probes™ Inc., Eugene, OR, USA) in LoFlo HL-5 for 2 hours in the dark. Excess stain solution was decanted and unbound MitoTracker Red was washed off the cells with 4 gentle washes with the Lo-Flo HL-5 over a 2 hr period in the dark with shaking on an orbital shaker (150 rpm) between washes. Lo-Flo HL-5 also reduces autofluorescence from the HL-5 medium [17]. After washing the stained cells, they were fixed for 15 min in 3.7% paraformaldehyde in PBS (12 mM Na_2HPO_4, 12 mM NaH_2PO_4, pH 6.5) and the fixed cells were washed with PBS 4 times for 5 min. The cells were mounted on clean glass slides with mounting solution (2.6% Dabco in 90% Glycerol and 10% PBS) and sealed. The mounted slide was viewed in a conventional fluorescence microscope (Olympus BH-2 or BX-50) and confocal microscope at the Confocal Microscopy Facility, Deakin University, Melbourne, Australia and images of AX2 and HPF representative cells were captured and analysed.

2.8. AMPK Subcellular Localisation Assay

Our present work focuses on determining the cellular localization of the Dictyostelium AMPK using fluorescent fusion proteins driven by the heterologous actin 15 (Act15) or Dictyostelium actin 6 promoter promoter. Axenically growing AX2 or strains vegetative cells were harvested, washed and fixed for 15 min in 3.7% paraformaldehyde in PBS. The fixed cells were washed with PBS 4 × 5 min. The cells were then permeabilised by incubating them in 0.1% - 0.5% Triton X-100 in PBS for 5 min and washed 4 × 5 min in PBS. The fixed and permeabilised cells were blocked for 3 hr at 4˚C, incubated overnight in primary antibody 500-fold dilution of AMPK antipeptide antibody in blocking buffer (Roche Diagnostics, Mannheim Germany) at 4 ˚C and washed 4 × 5 min at 21˚C ± 2˚C in PBS containing 0.05% Tween20. The cells were then treated for 45 min at 21˚C ± 2˚C with goat anti-rabbit Alexa-Flour 488-conjugated IgG antibody (Molecular Probes™ Inc., Eugene, OR, USA) using a 1:2000 dilution in blocking buffer. Finally, the cells were washed 4 × 5 min with PBS containing 0.05% tween 20, air dried for 5 min, mounted on clean glass slides with mounting solution (2.6% Dabco in 90% Glycerol and 10% PBS) and sealed. The mounted slide was viewed in a conventional fluorescence microscope (Olympus BH-2 or BX-50) and images of AX2 and HPF representative cells were captured and analysed.

2.9. Statistics

Results are shown as means ± SD. Bonferroni tests for multiple statistical comparisons and online supplment and Student's *t*-test (two-tailed) for unpaired samples were carried out to identify significant differences. For each experiment, all test results were compared with the control. R^2 is the coefficient of variation and equals the square of the Pearson product-moment correlation coefficient. The significance probability is the probability of the observed results occurring under the null hypothesis that the correlation coefficient was zero.

3. Results

The AMPK α subunit in Dictyostelium is encoded by a 2.6 kb single gene annotated as Q9XYP6 (www.expasy.org), AF118151 (www.ncbi.nlm.nih.gov/entrez) and DDB0215396 (http://www.dictybase.org/blast); comprised of five exons and four introns [9]. The N-terminus holds a highly conserved catalytic core, S_TKc domain and identical APE and DFG motifs with other eukaryotic cells (**Figure 1**).

3.1. Plasmid Copies and RNA Expression

The form of the AMPK α subunit that was over expressed contained the entire catalytic domain but was truncated within the putative region responsible for autoinhibition and binding to the β subunit. The truncation of the AMPK α subunit in the catalytic domain created a constitutively active form of AMPK. Southern blot analysis for the strains over expressing truncated AMPK α subunit and strains in which AMPK is antisense inhibited yielded bands that varied in their intensities (**Figure 2(A)** and **Figure 3(A)**). This indicates different plasmid copies of the respective strains. The least prominent band showed intensity higher than AX2 the wild type strain (**Figure 2(A)** and **Figure 3(A)**).

The transformants exhibited a characteristic, stable level of RNA expression and the differences reflected the expression vector copy numbers insertions in the genome. Both plasmid constructs affected expression in the

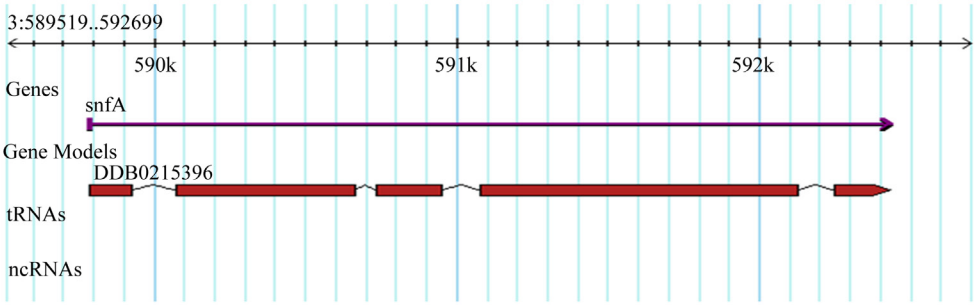

(a)

```
|Q9XYP6|Q9XYP6_DICDI ------MSPYQQNPIGSLGGLYGSGGIEKSSQIIGNYRLDKTLGIGSFGK  44
|Q38997|KIN10_ARATH  DEFNLVSSTIDHRIFKSRMDGSGTGSRSGVESILPNYKLGRTLGIGSFGR  55
|P54645|AAPK1_RAT    ----------------------MAEKQKHDGRVKIGHYILGDTLGVGTFGK  30
|Q13131|AAPK1_HUMAN  ----------------------MATAEKQKHDGRVKIGHYILGDTLGVGTFGK  32
|Q5EG47|AAPK1_MOUSE  ----------------------MAEKQKHDGRVKIGHYILGDTLGVGTFGK  30
|Q5U118|Q5U118_DROME ---------MPQMRAAAAEAVAAGSANGQPLVKIGHYLLGATLGTGTFGK  41
|Q95ZQ4|AAPK2_CAEEL  RKDRDSTDNSSKMSSPGGETSTKQQQELKAQIKIGHYILKETLGVGTFGK 100
|P06782|SNF1_YEAST   HHHHHHHHHHHHGHGGSNSTLNNPKSSLADGAHIGNYQIVKTLGEGSFGK  68
                                          : :* :  *** *:**:

|Q9XYP6|Q9XYP6_DICDI CHHMVVHRDLKPENLLLDPINKCIKIADFGLSNMMQDGDFLKTSCGSPN 194
|Q38997|KIN10_ARATH  CHRNMVVHRDLKPENLLLDSK-CNVKIADFGLSNIMRDGHFLKTSCGSPN 204
|P54645|AAPK1_RAT    CHRHMVVHRDLKPENVLLDAH-MNAKIADFGLSNMMSDGEFLRTSCGSPN 179
|Q13131|AAPK1_HUMAN  CHRHMVVHRDLKPENVLLDAH-MNAKIADFGLSNMMSDGEFLRTSCGSPN 181
|Q5EG47|AAPK1_MOUSE  CHRHMVVHRDLKPENVLLDAH-MNAKIADFGLSNMMSDGEFLRTSCGSPN 179
|Q5U118|Q5U118_DROME CHRHMIVHRDLKPENLLLDHN-MHVKIADFGLSNMMLDGEFLRTSCGSPN 190
|Q95ZQ4|AAPK2_CAEEL  CHRHMVVHRDLKPENLLLDEQ-NNVKIADFGLSNIMTDGDFLRTSCGSPN 249
|P06782|SNF1_YEAST   CHRHKIVHRDLKPENLLLDEH-LNVKIADFGLSNIMTDGNFLKTSCGSPN 206
                     **:: :*********:***       *********:* **.**:*******

|Q9XYP6|Q9XYP6_DICDI YAAPEVISGKLYAGPEVDVWSCGVILYAFLCAKLPFDDESIPMLFKKIRE 244
|Q38997|KIN10_ARATH  YAAPEVISGKLYAGPEVDVWSCGVILYALLCGTLPFDDENIPNLFKKIKG 254
|P54645|AAPK1_RAT    YAAPEVISGRLYAGPEVDIWSSGVILYALLCGTLPFDDDHVPTLFKKICD 229
|Q13131|AAPK1_HUMAN  YAAPEVISGRLYAGPEVDIWSSGVILYALLCGTLPFDDDHVPTLFKKICD 231
|Q5EG47|AAPK1_MOUSE  YAAPEVISGRLYAGPEVDIWSSGVILYALLCGTLPFDDDHVPTLFKKICD 229
|Q5U118|Q5U118_DROME YAAPEVISGKLYAGPEVDIWSCGVILYALLCGTLPFDDEHVPTLFRKIKS 240
|Q95ZQ4|AAPK2_CAEEL  YAAPEVISGKLYAGPEVDVWSCGVILYALLCGTLPFDDEHVPSLFRKIKS 299
|P06782|SNF1_YEAST   YAAPEVISGKLYAGPEVDVWSCGVILYVMLCRRLPFDDESIPVLFKNISN 256
                  **********:*********:**.*****.:**  *****: :* **::*
```

(b)

Figure 1. (a) Scaled map of genomic region encompassing AMPK α subunit (Chromosome 3 coordinates 589784-592434, Watson strand) (Dicty Base http://dictybase.org/gene/DDB_G0277905). The AMPK α subunit in Dictyostelium is encoded by a 2.65 kb gene; comprised of 5 exons and 4 introns. (b) The AMPK α subunit amino acids sequences of *Dictyostelium discoideum* using CLUSTAL W sequence alignment program (http://expasy.org) showed 61% homology to mammalian cells (*Homo sapiens* & *Rattus norvegicus*), 56% to *Drosophila melaogaster*, 61% to *Caenorhabditis elegans*, 65% to *Arabidopsis thaliana* and 64% to *Saccharomyces cerevisiae.* The N-terminus contains a highly conserved catalytic core, S TKc domain and identical APE (shaded blue) and DFG (shaded purple) motifs with other eukaryotic cells. The residue (tyrosine, Y) shaded pink is conserved and marks the start of the catalytic domain in all eukaryotes. The asterisk (*) means residues are identical in all sequences in the alignment. The colon (:) means conservative substitutions are present *i.e.* residues are identical or replaced by amino acids with similar biochemical properties. The period (.) means partially conservative substitutions of similar amino acids. The residue asparagine (N) at position 166 is present only in *D. discoideum.* Residue numbers to the right of the figure. Each amino acid residue is represented with one letter code.

expected copy number-dependent manner. A steady state level of AMPK α^{380} mRNA in quantitative northern blots tightly correlated with the plasmid copies of the AMPK α^{380} expression construct insertions in the strain genomes (**Figure 2**). Overexpression mutants showed strong RNA expression signals of increasing intensities as the copy number of AMPK α^{380} construct increased (**Figure 2**). The sense RNA fragment in pPROF361, was also expressed at high levels and tightly correlated with the plasmid copies (**Figure 3(B)**). By comparison with the sense RNA controls the equivalent antisense RNA levels were dramatically reduced even at the lowest plasmid copies of the antisense construct (**Figure 3**). Interestingly, the extent of RNA reduction correlated with the

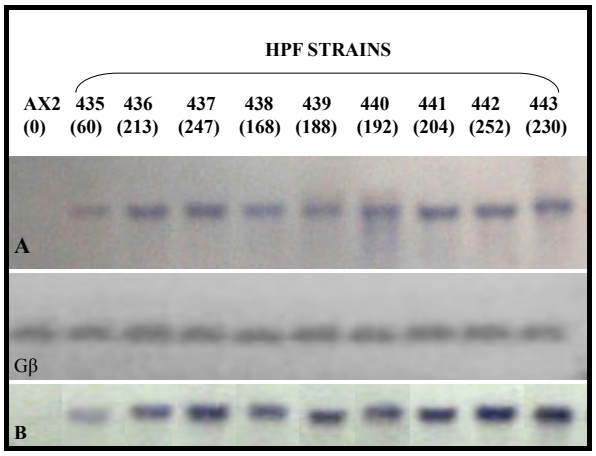

Figure 2. The plasmid copy number-dependent steady state RNA expression levels of the AMPK *α* subunit in overexpression strains. Genomic DNA and total RNA were extracted from stable transformants bearing plasmid expression vector construct (pPROF392) expressing the truncated catalytic domain of the AMPK α subunit (α^{380}). Figures atop the Southern blot indicate HPF strain identification number. Copy numbers for pPROF392 are indicated in parentheses. (A) Genomic DNA from *D. discoideum* AX2 and overexpression strains (HPF434-HPF442) were digested with *Eco*RI and subjected to electrophoresis on 1% agarose gel, blotted onto nylon membrane and probed with DIG-labelled AMPK *α* subunit DNA fragment. The different bands (1.14 kb) showing different intensities represent each strain indicating there are variations in the copies of the overexpression plasmid construct (pPROF392) insertions in the genome. The lower panel shows same genomic DNA probed with GTP-binding protein (β subunit) probe (1.77 kb), served as indicator that similar concentrations of the genomic DNA were used per strain. (B) Total RNA (1.14 kb) from corresponding strains were separated in a formaldehyde agarose gel, transferred onto nylon membrane and probed with DIG-labelled AMPK *α* subunit DNA. The blot shows RNA expression levels in the respective strains are closely related to the copy numbers. Endogenous transcript is not detectable with the probe in northern blot.

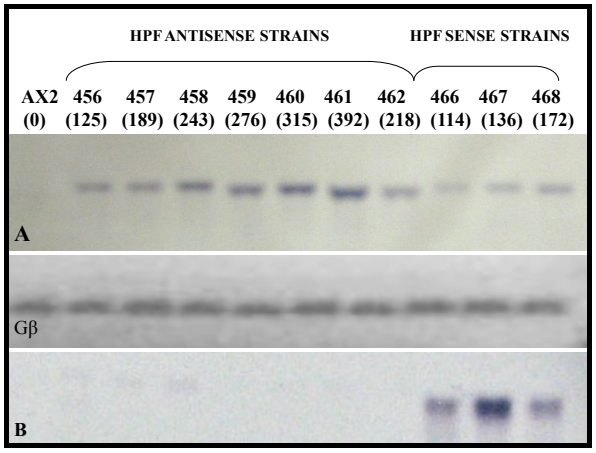

Figure 3. The plasmid copy number-dependent steady state RNA expression levels of the AMPK *α* subunit antisense plasmid construct in stable transformants evaluated by northern blotting. Genomic DNA and total RNA were extracted from stable transformants bearing plasmid expression vector constructs expressing the antisense RNA (pPROF362) complementary to part of the catalytic domain of the AMPK *α* subunit and the sense control strains. Figures atop the Southern blot indicate HPF strain identification number. Copy numbers pPROF362 are indicated in parenthesis. (A) Genomic DNA from *D. discoideum* AX2 and antisense inhibited strains (HPF456-HPF462) and complimentary sense strains (HPF466-HPF468) were digested with *Eco*RI and subjected to electrophoresis on 1% agarose gel, blotted onto nylon membrane and probed with DIG-labelled AMPK *α* subunit DNA fragment. The different bands (1.172 kb) showing varying intensities for each strain indicate there are variations in the copies of the antisense plasmid construct (pPROF362) and the control sense plasmid construct (pPROF361) insertions in the genome. The lower panel shows the same genomic DNA probed with GTP-binding protein (*β* subunit) probe (1.77 kb), served as indicator that similar concentrations of the genomic DNA were used per strain. (B) Total RNA from respective strains were separated in formaldehyde agarose gel, transferred onto nylon membrane and probed with DIG-labelled AMPK *α* subunit DNA. The blot shows RNA expression levels in the respective strains are closely related to the copy numbers. Endogenous transcript is not detectable with the probe in northern blot.

plasmid copies of the antisense RNA-expression construct (**Figure 3** and **Figure 4**). This indicates probable degradation in the antisense RNA expressing strains of both the antisense and the native mRNA. This would mean lower expression levels of the native mRNA. Additionally, the extent of elevation (overexpression) or reduction (antisense) of RNA levels tightly correlated with the plasmid copy number (**Figure 4**). Accordingly, the plasmid copies of the corresponding constructs were used as AMPK α subunit expression index.

3.2. Mitochondrial Mass Assay

The mitochondria mass and localisation in the strains tested was assayed with MitoTracker green and MitoTracker red. The MitoTracker red stained only the mitochondria; and more stain intensity with higher mitochondrial mass (**Figure 6**). The overexpression of the AMPK α catalytic domain resulted in more mitochondrial signals that were more intense per cell, whereas AMPK α antisense inhibition exhibited lesser signal compared to that of AX2 cells (**Figure 5** and **Figure 6**). Additionally, there was 2 - 3 fold increase in mitochondrial signals in strains overexpressing AMPK α subunit compared to AX2 (**Figure 6**). The mitochondrial fluorescence signal increase in AMPK α^{380} overexpression strains in relation to AX2 was assayed using the 530 nm filter in a Storm860^{TM} Fluoroimager (Amersham Biosciences, Castle Hill, Sydney, Australia) and analysed using the Image Quant tool (TLv2003.03) software (data not shown). The MitoTracker Green stain showed increased mitochondrial fluorescence in AMPK α^{380} overexpression strains but reduced in AMPK α subunit antisense strains compared AX2 (**Figure 5**). Increased intensity of MitoTracker Green stain in AMPK α^{380} strains signify elevated mitochondrial mass per cell. The higher the plasmid copies in the constitutively active AMPK strain the more the fluorescence from the assayed cells (**Figure 5** and **Figure 6**). The increase in mitochondrial mass is indicative of mitochondrial proliferation. In the same vein, the severe the antisense inhibition, the more apparent the mitotracker fluorescence decrease became (**Figure 5**).

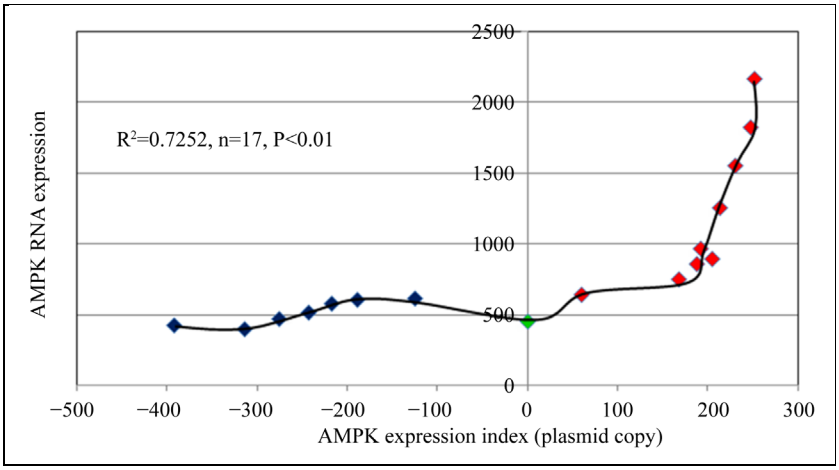

Figure 4. AMPK α subunit RNA expression patterns in overexpression and antisense-inhibited strains relative to wild type AX2. The red squares represents strains carrying the indicated number of copies of the AMPK α^{380} overexpression construct while blue squares represent strains carrying the indicated number of copies of an AMPK α subunit antisense construct per genome. The green square represents AX2, the wild type parental strain used as control. Overexpression of the truncated AMPK α subunit (AMPK α^{380}) RNA or antisense inhibition of the AMPK α subunit RNA as a function of the plasmid copies per genome was assayed by blotting with enhanced chemifluorescence substrate and the Storm860 phosphorimager. RNA expression tightly correlated with the copy numbers in each strain. To facilitate analysis and presentation of the data, positive values were assigned to plasmid copies for over expression constructs while negative values for the AMPK α antisense construct as expression indices. Antisense construct exerts a negative effect on expression of the native AMPK α subunit mRNA. R^2 is the coefficient of variation and equals the square of the Pearson product-moment correlation coefficient. The significance probability is the probability of the observed results occurring under the null hypothesis that expression levels and copy number were not correlated.

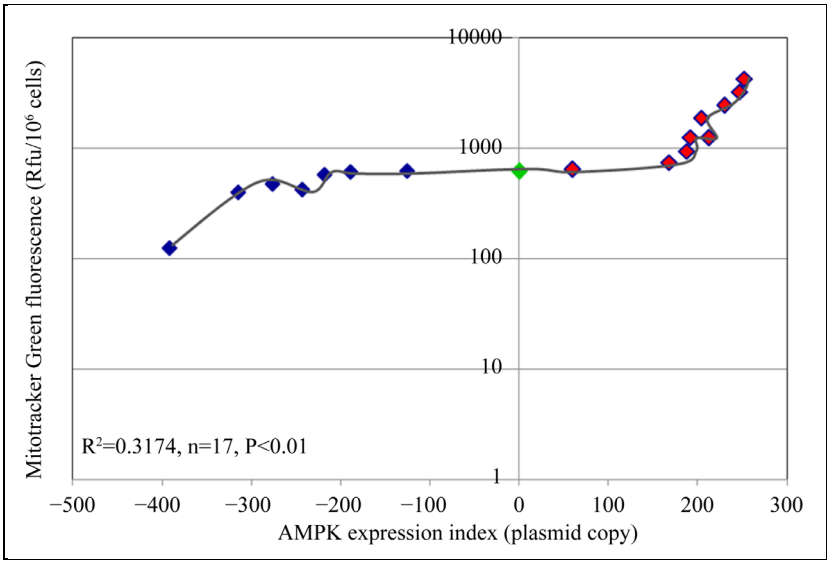

Figure 5. Effect of AMPK α subunit expression on mitochondrial mass in *Dictyostelium*. Mitochondrial "mass" was measured by fluorescence with the mitochondrion-specific dye, MitoTracker Green after subtraction of autofluorescence from unstained cells and presented as relative fluorescence units per 10^6 cells. The red squares represent individual strains each carrying the indicated number of copies of the AMPK α^{380} overexpression construct and blue squares for strains carrying the indicated number of copies of AMPK α subunit antisense construct. The green square represent the AX2, the wild type parental strain used as control. R^2 is the coefficient of variation and equals the square of the Pearson product-moment correlation coefficient. The significance probability is the probability of the observed results occurring under the null hypothesis that the correlation coefficient was zero. Negative values indicate the copy numbers of the AMPK α subunit antisense inhibition construct, while positive values indicate copy numbers of the overexpression construct.

3.3. AMPK Subcellular Localisation in *Dictyostelium*

The AX2 and HPF strains were used to study the subcellular localization of AMPK. AMPK α was cytosolic in AX2 and the HPF strains (**Figure 6**). The AMPK α subunit distribution showed sequestration smooth homogeneity within the cytosol, less densely to the cell membranes and does not seem to localize to particulate cellular sites in AX2 cell (**Figure 6(a)**) and HPF strains (**Figure 6(b)**, **Figure 6(c)**). Truncation of the α subunit at the 380 amino acid residue position to yield a constitutively active segement or at 510 position did not affect distribution or whether experimental tools discriminate between the cytoplasmic and nuclear pools of AMPK (**Figure 6(b)**). Constitutive activation or antisense inhibition of the subunit did not affect the subcellular localization (**Figures 6(b)** and **Figure 6(c)**). The same localization patterns were seen in growing cells of both the wild type and strains. The α subunit was not present in the mitochondria. This is evident in that the overlay did not portray this fact (**Figure 6**). This finding supports the earlier hypothesis that if AMPK was the proximal regulator of mitochondrial biogenesis it then would not be present in the mitochondria [9].

4. Discussion

AMPK has been the focus of increasing attention for its fundamental roles in cellular energy homeostasis in healthy cells and in a variety of pathological situations, most notably diabetes, cancer [1] [18] and mitochondrial diseases [7]. The activated cascade regulates metabolic pathways and promotes the adaptation of eukaryotic cells to the ever changing microenvironment [1] [19]. Thus, AMPK functions as a metabolic masterswitch, or more accurately, "low fuel warning system" in mammalian [1] [18] and other eukaryotic cells [20]-[22]. Thus places AMPK holoenzyme at a central control point in maintaining cellular energy homeostasis. This pivotal role places AMPK in an ideal position to also play a wider role in regulating whole-body energy metabolism [23]. Furthermore, AMPK regulates the expression of a large number of genes, the stability of several mRNAs,

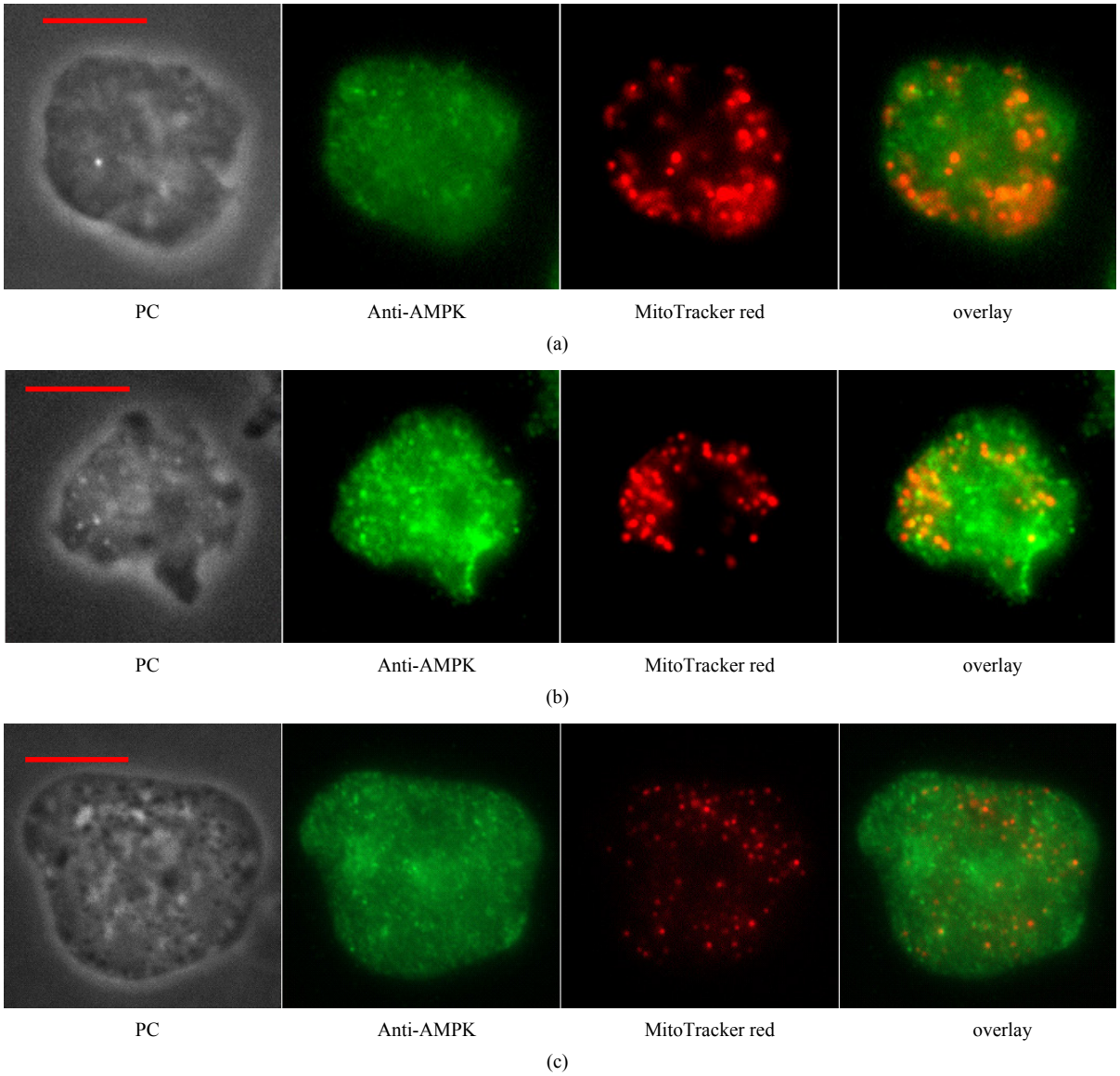

Figure 6. Localisation of AMPK *α* subunit in *Dictyostelium* cells. The vegetative cells were stained with MitoTracker red and probed with antipeptide antibody followed by Alexa-Flour 488-conjugated anti-rabbit IgG. Fluorescence was visualised with a Zeiss Axioplan fluorescent microscope and all images were captured at X1000 magnification. The green indicate AMPK localisation and red represents mitochondrial localisation in the cytoplasm. (a) AX2 cells; (b) overexpression mutant; (c) antisense inhibited mutant. The red bar in the panels represents ~0.5 µm. PC – phase contrast.

cell polarity, and mitosis [24]-[26]. Access to and modification of these substrates requires cytoplasmic localization of AMPK. Moreover, the oxidative cellular function will require a ubiquitous system and may coordinately regulate response to metabolic requirements.

In *Dictydstelium*, AMPK cascade have putative heteromeric forms and cytosolic localization patsterns. AMPK *α* remain cytosolic in location. Moreover, the developmental phases of the life cycle will support the cytosolic localization; and since the organelles are potentially reorganized or removed entirely during transitions from vegetative living to fruiting body morphology. Cytosolic subcellular localization of *Dictyostelium snf*A is not surprising given the extensive number of roles AMPK having been documented to play in this organism. The observed intracellular distribution of the *snf*A provides a means to maintain appropriate intracellular and organellar distribution of AMPK. The less complexity of *Dictyostelium* will make do with one gene coding for each subunit and the cytosolic localization. In the mammalian cells, AMPK shuttles between the nucleus and the cy-

toplasm under normal growth conditions, a process that depends on the nuclear exporter Crm1 [27]. However, many factors control the distribution of AMPK [27] [28]. For instance, environmental stress, heat shock or oxidant exposure drive more nuclear localization of AMPK [27] [29]. Given their apparently common localisation, AMPK tends to stay in the cytosol whether modified or wild type. In mammals, the AMPK subunits are encoded by multiple genes and preferentially and differentially localise to either the cytoplasm or nuclei [30] [31]. However, nucleocytoplasmic shuttling does not take place in high-density cell cultures, for which AMPK is confined to the cytoplasm [27]. This is typical state of the vegetative cells during vigorous proliferation and attaining high density frequently.

The localization of AX2 and HPF strains of the α subunit are similar. However, *snf*A expression ias more intense in constitutively active strains than that observe in the AX2 but lesser in attenuation strains. Constitutive activation of AMPK via truncation of the catalytic domain with significant increased in activity of the AMPK approximates the persistent AMPK activation such as from stressors [7] [32]. Strains expressing the antisense construct contained varied plasmid copies and corresponding RNA expression profile depicting dimunition of RNA as the plasmid copies increased; portrays a scenario of *snf*A attenuation by mutations. This indicates degradation in the antisense RNA expressing transformants of both the antisense and the native mRNA. This will mean lower expression levels of the native mRNA. During successful antisense RNA inhibition both strands of the mRNA, antisense RNA duplex is degraded by the RISC complex [33]. Moreover, strains with higher plasmid copies of antisense plasmids show severe growth and development defects [7]. The localisation of the α of *snf*A suggests that it may have plethora of cytoplasmic functions. Together, this intracellular localization provides a unique set of tools to rapidly adjust the distribution of AMPK to changes in cell physiology. The importance of these concepts is becoming ever more evident as mechanisms of hormone and drug action are resolved to the subcellular location of their target molecules [34].

However, further studies needed to understand the importance and the dynamics of the compartmentalisation of the c2-AMPK complexes, focusing on specific interactions in each location. The need for isoform-selective activation of AMPK to develop cardioprotective therapies has been highlighted in a recent review article [35] and protein—protein interaction studies could result in new drug design that acts specifically on c2-AMPK complexes to ameliorate the disease caused by the PRKAG2 mutations.

Our study provides insight into the subcellular distribution of AMPK. Our results demonstrate that AMPK localization was steady in AX2 and derived strains whether constitutively active or antisense inhibited depicting extreme states of transformation.

Acknowledgements

We gratefully acknowledge the support by La Trobe University Postgraduate Research Scholarship (LTUPRS) and the Australian Government International Postgraduate Research Scholarship Scheme (IPRSS). The present study cannot have been completed without it.

References

[1] Hardie, D.G. and Hawley, S.A. (2001) AMP-Activated Protein Kinase: The Energy Charge Hypothesis Revisited. *BioEssays*, **23**, 1112-1119. http://dx.doi.org/10.1002/bies.10009

[2] Hardie, D.G. (2007) AMP-Activated/SNF1 Protein Kinases: Conserved Guardians of Cellular Energy. *Nature Reviews in Molecular Cell Biology*, **8**, 774-785. http://dx.doi.org/10.1038/nrm2249

[3] Rutter, G., Silva, A., Xavier, G. and Leclerc, I. (2003) Roles of 5'-AMP-Activated Protein Kinase (AMPK) in Mammalian Glucose Homeostasis. *Biochemical Journal*, **375**, 1-16. http://dx.doi.org/10.1042/BJ20030048

[4] Towler, M.C. and Hardie, D.G. (2007) AMP-Activated Protein Kinase in Metabolic Control and Insulin Signaling. *Circulation Research*, **100**, 328-341. http://dx.doi.org/10.1161/01.RES.0000256090.42690.05

[5] Viollet, B., Foretz, M., Guigas, B., Horman, S., Dentin, R., Bertrand, L., Hue, L. and Andreelli, F. (2006) Activation of AMP-Activated Protein Kinase in the Liver: A New Strategy for the Management of Metabolic Hepatic Disorders. *Journal of Physiology*, **574**, 41-53. http://dx.doi.org/10.1113/jphysiol.2006.108506

[6] Eichinger, L., Pachebat, J.A., Glockner, G., Rajandream, M.A., Sucgang, R., Berriman, M., Song, J., Olsen, R., Szafranski, K., Xu, Q., Tunggal, B., Kummerfeld, S., Madera, M., Konfortov, B.A., Rivero, F., Bankier, A.T., Lehmann, R., HamLin, N., Davies, R., Gaudet, P., Fey, P., Pilcher, K., Chen, G., Saunders, D., Sodergren, E., Davis, P., Kerhornou, A., Nie, X., Hall, N., Anjard, C., Hemphill, L., Bason, N., Farbrother, P., Desany, B., Just, E., Morio, T., Rost, R.,

Churcher, C., Cooper, J., Haydock, S., van Driessche, N., Cronin, A., Goodhead, I., Muzny, D., Mourier, T., Pain, A., Lu, M., Harper, D., Lindsay, R., Hauser, H., James, K., Quiles, M., Madan Babu, M., Saito, T., Buchrieser, C., Wardroper, A., Felder, M., Thangavelu, M., Johnson, D., Knights, A., Loulseged, H., Mungall, K., Oliver, K., Price, C., Quail, M.A., Urushihara, H., Hernandez, J., Rabbinowitsch, E., Steffen, D., Sanders, M., Ma, J., Kohara, Y., Sharp, S., Simmonds, M., Spiegler, S., Tivey, A., Sugano, S., White, B., Walker, D., Woodward, J., Winckler, T., Tanaka, Y., Shaulsky, G., Schleicher, M., Weinstock, G., Rosenthal, A., Cox, E.C., Chisholm, R.L., Gibbs, R., Loomis, W.F., Platzer, M., Kay, R.R., Williams, J., Dear, P.H., Noegel, A.A., Barrell, B. and Kuspa, A. (2005) The Genome of the Social Amoeba *Dictyostelium discoideum*. *Nature*, **435**, 43-57. http://dx.doi.org/10.1038/nature03481

[7] Bokko, B.P., Said, F., Bandala, E., Ahmed, A., Annesely, S.J., Huang, X., Khurana, T., Kimmel, A.R. and Fisher, P.R. (2007) Diverse Cytopathologies in Mitochondrial Disease Are Caused by AMPK. *Molecular Biology of the Cell*, **18**, 1874-1886. http://dx.doi.org/10.1091/mbc.E06-09-0881

[8] Sung, S., Bisson, S., Koehler, S. and Podgorski, G.J. (1999) The *Dictyostelium* snf1/AMP-Activated Kinase. Unpublished, EMBL/GenBank ID AF118151.

[9] Bokko, B.P., Ahmed, A.U. and Fisher, P.R. (2014) Constitutive Activation of AMP-Activated Protein Kinase (AMPK) Propel Mitochondrial Biogenesis. *Journal of Cell Biology and Genetics*, **4**, 15-26. http://dx.doi.org/10.5897/JCBG2013.0037

[10] Watts, D.J. and Ashworth, J.M. (1970) Growth of Myxameobae of the Cellular Slime Mould *Dictyostelium discoideum* in Axenic Culture. *Biochemical Journal*, **119**, 171-174.

[11] Nellen, W., Silan, C. and Firtel, R.A. (1984) DNA-Mediated Transformation in *Dictyostelium discoideum*: Regulated Expression of an Actin Gene Fusion. *Molecular Cell Biology*, **4**, 2890-2898.

[12] Fey, P., Compton, K. and Cox, E. (1995) Green Fluorescent Protein Production in the Cellular Slime Molds *Polysphondylium pallidum* and *Dictyostelium. Gene*, **165**, 127-130. http://dx.doi.org/10.1016/0378-1119(95)00430-E

[13] Levi, S., Polyakov, M. and Egelhoff, T.T. (2000) Green Fluorescent Protein and Epitope Tag Fusion Vectors for *Dictyostelium discoideum*. *Plasmid*, **44**, 231-238. http://dx.doi.org/10.1006/plas.2000.1487

[14] Damer, C.K., Bayeva, M., Hahn, E.S., Rivera, J. and Socec, C.I. (2005) Copine A, a Calcium-Dependent Membrane-Binding Protein, Transiently Localizes to the Plasma Membrane and Intracellular Vacuoles in Dictyostelium. *BMC Cell Biology*, **6**, 46. http://dx.doi.org/10.1186/1471-2121-6-46

[15] Kirsten, J.H., Xiong, Y., Davis, C.T. and Singleton, C.K. (2008) Subcellular Localization of Ammonium Transporters in *Dictyostelium discoideum*. *BMC Cell Biology*, **9**, 71. http://dx.doi.org/10.1186/1471-2121-9-71

[16] Witke, W., Nellen, W. and Noegel, A. (1987) Homologous Recombination in the *Dictyostelium* α-Actin Gene Leads to an Altered mRNA and Lack of the Protein. *EMBO Journal*, **6**, 4143-4148.

[17] Liu, T., Mirschberger, C., Chooback, L., Arana, Q., Dal Sacco, Z., MacWilliams, H. and Clarke, M. (2002) Altered Expression of the 100 kDa Subunit of the *Dictyostelium* Vacuolar Proton Pump Impairs Enzyme Assembly, Endocytic Function and Cytosolic pH Regulation. *Journal of Cell Science*, **115**, 1907-1918.

[18] Winder, W.W. and Hardie, D.G. (1999) AMP-Activated Protein Kinase, a Metabolic Master Switch: Possible Roles in Type 2 Diabetes. *American Journal of Physiology*, **277**, E1-E10.

[19] Suzuki, A., Okamoto, S., Lee, S., Saito, K., Shiuchi, T. and Minokoshi, Y. (2007) Leptin Stimulates Fatty Acid Oxidation and Peroxisome Proliferator-Activated Receptor Alpha Gene Expression in Mouse C2C12 Myoblasts by Changing the Subcellular Localization of the Alpha2 form of AMP-Activated Protein Kinase. *Molecular Cell Biology*, **27**, 4317-4327. http://dx.doi.org/10.1128/MCB.02222-06

[20] Wilson, W.A., Hawley, S.A. and Hardie, D.G. (1996) The Mechanism of Glucose Repression/Derepression in Yeast: SNF1 Protein Kinase Is Activated by Phosphorylation under Derepressing Conditions, and This Correlates with a High AMP:ATP Ratio. *Current Biology*, **6**, 1426-1434. http://dx.doi.org/10.1016/S0960-9822(96)00747-6

[21] Carlson, M. (1999) Glucose Repression in Yeast. *Current Opinions in Microbiology*, **2**, 202-207. http://dx.doi.org/10.1016/S1369-5274(99)80035-6

[22] Pan, D.A. and Hardie, D.G. (2002) A Homologue of AMP-Activated Protein Kinase in *Drosophila melanogaster* Is Sensitive to AMP and Is Activated by ATP Depletion. *Biochemistry Journal*, **367**, 179-186. http://dx.doi.org/10.1042/BJ20020703

[23] Carling, D. (2004) The AMP-Activated Protein Kinase Cascade—A Unifying System for Energy Control. *Trends in Biochemical Science*, **29**, 18-24. http://dx.doi.org/10.1016/j.tibs.2003.11.005

[24] Yang, W., Hong, Y.H., Shen, X., Frankowski, C., Camp, H.S. and Leff, T. (2001) Regulation of Transcription by AMP-Activated Protein Kinase. *Journal of Biological Chemistry*, **276**, 38341-38344. http://dx.doi.org/10.1074/jbc.C100316200

[25] Eberhardt, W., Doller, A., Akool, E. and Pfeilschifter, J. (2007) Modulation of mRNA Stability as a Novel Therapeutic Approach. *Pharmacology and Therapeutics*, **114**, 56-73. http://dx.doi.org/10.1016/j.pharmthera.2007.01.002

[26] Lee, J.H., Koh, H., Kim, M., Kim, Y., Lee, S.Y., Lee, S., Shong, J., Kim, J., Chung, J. and Karess, R.E. (2007) Energy-Dependent Regulation of Cell Structure by AMP-Activated Protein Kinase. *Nature*, **447**, 1017-1021. http://dx.doi.org/10.1038/nature05828

[27] Kodiha, M., Rassi, J.G., Brown, C.M. and Stochaj, U. (2007) Localization of AMP Kinase Is Regulated by Stress, Cell Density, and Signaling through the MEK→ERK1/2 Pathway. *American Journal of Physiology—Cell Physiology*, **293**, C1427-C1436. http://dx.doi.org/10.1152/ajpcell.00176.2007

[28] Salt, I.P., Celler, J.W., Hawley, S.A., Prescott, A., Woods, A., Carling, D. and Hardie, D.G. (1998) AMP-Activated Protein Kinase—Greater AMP Dependence, and Preferential Nuclear Localization, of Complexes Containing the α2 Isoform. *Biochemical Journal*, **334**, 177-187.

[29] Kodiha, M., Chu, A., Matusiewicz, N. and Stochaj, U. (2004) Multiple Mechanisms Promote the Inhibition of Classical Nuclear Import upon Exposure to Severe Oxidative Stress. *Cell Death and Differentiation*, **11**, 862-874. http://dx.doi.org/10.1038/sj.cdd.4401432

[30] Turnley, A.M., Stapleton, D., Mann, R.J, Witters, L.A., Kemp, B.E. and Bartlett, P.F. (1999) Cellular Distribution and Developmental Expression of AMP-Activated Protein Kinase Isoforms in Mouse Central Nervous System. *Journal of Neurochemistry*, **72**, 1707-1716. http://dx.doi.org/10.1046/j.1471-4159.1999.721707.x

[31] Pinter, K., Grignani, R.T., Watkins, H. and Redwood, C. (2013) Localisation of AMPK γ Subunits in Cardiac and Skeletal Muscles. *Journal of Muscle Research and Cell Motility*, **34**, 369-378. http://dx.doi.org/10.1007/s10974-013-9359-4

[32] Crute, B.E., Seefeld, K., Gamble, J., Kemp, B.E. and Witters, L.A. (1998) Functional Domains of the α1 Catalytic Subunit of the AMP-Activated Protein Kinase. *Journal of Biological Chemistry*, **273**, 35347-35354. http://dx.doi.org/10.1074/jbc.273.52.35347

[33] Hinas, A. and Söderbom, F. (2007) Treasure Hunt in an Amoeba: Non-Coding RNAs in *Dictyostelium discoideum*. *Current Genetics*, **51**, 141-159. http://dx.doi.org/10.1007/s00294-006-0112-z

[34] Creighton, J. (2011) Targeting Therapeutic Effects: Subcellular Location Matters. Focus on "Pharmacological AMP-Kinase Activators Have Compartment-Specific Effects on Cell Physiology". *American Journal of Physiology Cell Physiology*, **301**, C1293-C1295. http://dx.doi.org/10.1152/ajpcell.00358.2011

[35] Kim, M. and Tian, R. (2011) Targeting AMPK for Cardiac Protection: Opportunities and Challenges. *Journal of Molecular and Cellular Cardiology*, **51**, 548-553. http://dx.doi.org/10.1016/j.yjmcc.2010.12.004